8

# A Novel Implicit Adaptive zero pole-placement PID Controller

*Ali Zayed and **Mahmoud ELFandi
*The 7th of Aperial University, Libya. **Alfateh University, Libya

## 1. Introduction

For most simple processes, PID control can provide satisfactory closed loop performance. However, in spite of the considerable advantages of conventional PID controllers (such as simplicity of their structures, robustness and ease of implementation), they still have a major drawback in that the controllers may need to be re-tuned, if the systems to be controlled are subjected to significant changes, in order to achieve satisfactory performance. For this reason, during the last two decades much work in linear control theory has been devoted to incorporating the flexibility of self-tuning control and the simplicity of PID structures. A lot of self-tuning methods have been developed and special attention is currently being paid to PID self-tuning controllers and their implementation, [e.g. Yusof R. & et al., (1994); Yusof, R.; (1993) and Tokuda M.; & Yamamoto T.; (2002)].

During the past three decades, a special attention has also been given to the problem of designing pole-placement controllers and self-tuning regulators. Various self-tuning controllers based on classical pole-placement ideas were developed and employed in real applications, [e.g. Sirisena H. & Teng F.,(1986); Zhu Q., & et al., (2002); Zayed A. & Hussain A., (2004); Astrom K.., & Wittenmark B., (1973)]. The popularity of pole-placement techniques may be attributed to the fact that in the regulator case they provide mechanisms to over-come the restriction to minimum-phase plants of the original minimum variance self-tuner of Astrom K., & Wittenmark B., (1973). In the servo case, they provide the ability to directly introduce bandwidth and damping ratio as tuning parameters. In addition, there is some improvement in robustness of pole-placement methods, as they simply modify the system dynamics as opposed to cancelling them as per the early optimal self-tuning controllers. Furthermore, unlike many of the self-tuning based PID control designs [see for example Yusof R. & et al., (1994); Yusof, R.; (1993)], in which the tuning parameters must be selected using a trial and error procedure, the tuning parameters for pole-placement controllers can be automatically set *on-line* by specifying the desired closed loop poles.

Comparatively, only little attention has been given to zeros since they are considered to be less crucial than poles. Most of the previous discussion on zeros are centred around the choice of the sampling time so that the resulting system is invertible. However, it is important to note that zeros may be used to achieve better set point tracking Zayed A. & Hussain A., (2004)., and they may also help reduce the magnitude of the control action Sirisena H. & Teng F.,(1986)..

Therefore, in order to achieve more effective control action and combine the advantages of the self-tuning controllers with those of the PID, and zero pole-placement controllers need to be integrated. However, the most of multivariable pole-placement controllers are explicit and have considerable drawbacks in that the control designs involve the solution of a Diophantine equations, which in some applications may lead to excessive computational and numerical instability problems and they are obtained as a right matrix-fraction and an additional transforming step from a right to left-matrix description is required in order to implement the control law Zhu Q., & et al., (2002).

In an attempt to avoid solving Diophantine equations and to obtain the control as a left matrix-fraction for direct implementation, a novel multivariable generalised minimum variance stochastic adaptive controller with PID pole placement structure is presented in this paper. It builds on the previous works Zhu Q., & et al., (2002); Zayed, A. & et al., (2004); and Zayed A. & Hussain A., (2004). The proposed design provides the designer with a choice of using either a self-tuning controller or an implicit PID controller.

The paper is organised as follows: the derivation of the control law is discussed in section 2. In section 3, a simulation case study is carried out in order to demonstrate the effectiveness of the proposed controller in the performance of the closed loop system. Finally, some concluding remarks are presented in section 4.

## 2. Derivation of control law

In deriving the multivariable self-tuning control law we assume that the process is described by the following Controlled Auto-Regressive Moving Average (CARMA) model Yusof R. & et al., (1994); Zayed, A. & et al., (2004); Astrom K.., & Wittenmark B., (1973):

$$\mathbf{A}(z^{-1})\mathbf{y}(t) = \mathbf{B}(z^{-1})\mathbf{u}(t-k) + \mathbf{C}(z^{-1})\xi(t) \tag{1}$$

where $\mathbf{y}(t)$ is the measured output vector with dimension ($n \times 1$), $\mathbf{u}(t)$ is the measured control input vector ($n \times 1$), $\xi(t)$ is an uncorrelated sequence of random variables with zero mean, *k* is the time delay in the integer sampling interval and $(t)$ denotes the sampling instant, $t = 1,2,3,.....,$.

The polynomial matrices $\mathbf{A}(z^{-1})$, $\mathbf{B}(z^{-1})$ and $\mathbf{C}(z^{-1})$ are expressed in terms of the backwards shift operator, $z^{-1}$ {i.e. $z^{-1}\mathbf{x}(t) = \mathbf{x}(t-1)$}, and are given as:

$$\mathbf{A}(z^{-1}) = \mathbf{I} + \mathbf{A}_1 z^{-1} + \mathbf{A}_2 z^{-2} + ............ + \mathbf{A}_{n_a} z^{-n_a} \tag{2}$$

$$\mathbf{B}(z^{-1}) = \mathbf{B}_0 + \mathbf{B}_1 z^{-1} + ...... + \mathbf{B}_{n_b} z^{-n_b} \quad , \mathbf{B}(0) \neq 0 \tag{3}$$

$$\mathbf{C}(z^{-1}) = \mathbf{I} + \mathbf{C}_1 z^{-1} + \mathbf{C}_2 z^{-2} + .......... + \mathbf{C}_{n_c} z^{-n_c} \tag{4}$$

where $n_a$, $n_b$, and $n_c$ are the degrees of the polynomials.

The coefficients of the above polynomials are ($n \times n$) matrices and $\mathbf{I}$ is the ($n \times n$) identity matrix.

It is assumed that the zeroes of the det $\mathbf{C}(z^{-1})$ lie inside the unit disc of the z-plane (that is, the polynomial $\mathbf{C}(z^{-1})$ is inverse stable). It is also assumed without any loss of generality, that the disturbance transfer function is proper (i.e. $n_c \le n_a$) [1, 4, 8]. No assumption concerning the polynomial $\mathbf{B}(z^{-1})$ is made implying that the process can be a minimum or non-minimum phase system.
The control law minimises the variance of an auxiliary output $\phi(t)$:

$$\varphi(t) = \mathbf{P}(z^{-1})\mathbf{y}(t) + \mathbf{Q}'(z^{-1})\mathbf{u}(t-k) - \mathbf{R}(z^{-1})\mathbf{w}(t-k) \tag{5}$$

Here $\mathbf{w}(t)$ is the $(n \times 1)$ set point vector and $\mathbf{P}(z^{-1})$, $\mathbf{Q}'(z^{-1})$ and $\mathbf{R}(z^{-1})$ are the user-defined transfer functions in the backward shift operator $z^{-1}$. $\mathbf{P}(z^{-1})$ is rational matrix which can be expressed as:

$$\mathbf{P}(z^{-1}) = \mathbf{P}_n(z^{-1})\mathbf{P}_d^{-1}(z^{-1}) \tag{6}$$

here $\mathbf{P}_n(z^{-1})$ and $\mathbf{P}_d(z^{-1})$ are respectively monic $(n \times n)$ numerator and denominator matrices with degrees $n_{p_n}$ and $n_{p_d}$. The performance of closed loop system is determined by the selection of the polynomial matrices $\mathbf{P}(z^{-1})$, $\mathbf{Q}'(z^{-1})$ and $\mathbf{R}(z^{-1})$ which are important design decisions.
The control law which minimises the above cost function given by (5) can be expressed as( Zayed, A. & et al., (2004)):

$$\mathbf{Q}_s\mathbf{u}(t) = [\mathbf{H}_0\mathbf{w}(t) - \bar{\mathbf{F}}_s'\mathbf{y}(t)] \tag{7}$$

where $\mathbf{Q}_s$ and $\mathbf{H}_0$ are the user transfer functions matrices which they depend on $\mathbf{Q}$ and $\mathbf{R}$, respectively.
We further assume that $\mathbf{Q}_s$ and $\mathbf{H}_0$ can also be expressed as:

$$\left.\begin{aligned} \mathbf{H}_0 &= \bar{\mathbf{F}}_s' \\ \mathbf{Q}_s &= \Delta(\tilde{\mathbf{H}}'\mathbf{V})^{-1}\bar{\mathbf{Q}}_s' \\ \Delta &= \Delta\mathbf{I} = (1 - z^{-1})\mathbf{I} \end{aligned}\right\} \tag{8}$$

$\Delta$ and $\bar{\mathbf{Q}}_s'$ are the $(n \times n)$ polynomial matrices, and $\mathbf{V}$ is a user-defined polynomial diagonal gain matrix. Here $\tilde{\mathbf{H}}'$ and $\mathbf{I}$ are the $(n \times n)$ desired closed loop system zeros polynomial matrix and identity matrix, respectively.
Combining equations (7) and (8), gives:

$$\Delta\bar{\mathbf{Q}}_s'\mathbf{u}(t) = [\mathbf{V}\bar{\mathbf{F}}_s'\mathbf{w}(t) - \tilde{\mathbf{H}}'\mathbf{V}\bar{\mathbf{F}}_s'\mathbf{y}(t)] \tag{9}$$

In this case,

$$\bar{\mathbf{Q}}'_s(z^{-1}) = \bar{\mathbf{Q}}'_{s0} + \bar{\mathbf{Q}}'_{s1} z^{-1} + \ldots\ldots + \bar{\mathbf{Q}}'_{sn_{\bar{Q}'_s}} z^{-n_{\bar{Q}'_s}} \tag{10}$$

It can clearly be seen from (8) that the polynomial $\bar{\mathbf{Q}}'_s$ and the gain $\mathbf{V}$ can be considered as user defined parameters since they depend on the user transfer function $\mathbf{Q}'(z^{-1})$.

We can see clearly from equations (8) and (9) that the controller denominator has now conveniently been split into two parts:

1. An integrator action part ($\Delta$) required for PID design
2. An arbitrary compensator ($\bar{\mathbf{Q}}'_s(z^{-1})$) that may be used for pole-placement placement design.

### 2.1 Multivariable Self-tuning PID Controller design (mode 1)

In this mode, the generalised minimum variance controller operates as a conventional self-tuning PID controller, which can be expressed in the most commonly used velocity form [1, 2] as:

$$\Delta\mathbf{u}(t) = [\mathbf{K_P} + \mathbf{K_I} + \mathbf{K_D}]\mathbf{e}(t) - [\mathbf{K_P} + 2\mathbf{K_D}]\mathbf{e}(t-1) + [\mathbf{K_D}]\mathbf{e}(t-2) \tag{11}$$

$$\mathbf{e}(t) = \mathbf{w}(t) - \mathbf{y}(t) \tag{12}$$

where $\mathbf{K_P}$, $\mathbf{K_I}$ and $\mathbf{K_D}$ are ($n \times n$) matrices denote the proportional gain, the integral gain and derivative gain respectively. $\Delta$ is the difference operator defined as:

In order to obtain a self-tuning controller with PID structure the control law in equation (9) must have the same form of as the PID controller in equation (11).

If we assume that the degree of polynomial $\bar{\mathbf{F}}'_s$ is equal to 2:

$$\bar{\mathbf{F}}'(z^{-1}) = \bar{\mathbf{F}}'_{s0} + \bar{\mathbf{F}}'_{s1} z^{-1} + \bar{\mathbf{F}}'_{s2} z^{-2} \tag{13a}$$

and if we set

$$\bar{\mathbf{Q}}'_s(z^{-1}) = \tilde{\mathbf{H}}' = \mathbf{I} \tag{13b}$$

and make use of equations (13a), (13b) and (9) a multivariable self-tuning controller with PID structure is obtained, where

$$\Delta\bar{\mathbf{Q}}'_s\mathbf{u}(t) = \mathbf{V}(\bar{\mathbf{F}}'_{s0} + \bar{\mathbf{F}}'_{s1} z^{-1} + \bar{\mathbf{F}}'_{s2} z^{-2})[\mathbf{w}(t) - \mathbf{y}(t)] \tag{14}$$

$$\mathbf{K_P} = -\mathbf{V}(\bar{\mathbf{F}}'_{s1} + 2\bar{\mathbf{F}}'_{s2}) \tag{15a}$$

$$\mathbf{K_I} = \mathbf{V}(\bar{\mathbf{F}}'_{s0} + \bar{\mathbf{F}}'_{s1} + \bar{\mathbf{F}}'_{s2}) \tag{15b}$$

$$\mathbf{K_D} = \mathbf{V}(\bar{\mathbf{F}}'_{s2}) \tag{15c}$$

As can be seen from equations (5) and (8)-(15) that the PID controller is tuned by a selection of the polynomial $\mathbf{P}$ and the gain $\mathbf{V}$ which must be selected in trial and error procedure.

Alternatively, these tuning parameters can be automatically and implicitly set on line by specifying the desired closed loop poles Zhu Q., & et al., (2002); Zayed A. & Hussain A., (2004).

### 2.2 New Implicit Multivariable PID Pole-placement Controller (Mode 2)

The generalised minimum variance control law given by equation (9) was extended to achieve explicit PID pole-zero placement by Zayed A., (1997); Zayed A., (2005) Zayed A.,& et al., (2006) and Zhu and Zhu Q., & et al., (2002). However, these explicit PID controller designs have two drawbacks in that the controllers involve the solution of Diophantine equation. In addition, the explicit designs have the right fraction structure and an additional transforming step from a right to left-matrix description is required in order to implement the control law. For this reasons the generalised minimum variance control is modified such that solving Diophantine is not considered in the design and has a left fraction structure enables direct implementation.. The controller may then be considered as an implicit controller in the sense that the control design step is trivial.

If we set the desired closed loop zeros matrix $\tilde{\mathbf{H}}' = \mathbf{I}$ , then the control law given by equation (9) can also expressed as follows:

$$\bar{\mathbf{q}}_s' \mathbf{u}(t) = [\mathbf{V}\bar{\mathbf{F}}_s'\mathbf{w}(t) - \mathbf{V}\bar{\mathbf{F}}_s'\mathbf{y}(t)] \tag{16}$$

where

$$\bar{\mathbf{q}}_s' = \Delta\bar{\mathbf{Q}}_s' \tag{17}$$

By combining equations (16) and (1), the closed loop transfer function is obtained as:

$$\mathbf{y}(t) = (\mathbf{A} + z^{-k}\mathbf{B}[\bar{\mathbf{q}}_s']^{-1}\mathbf{V}\bar{\mathbf{F}}_s')^{-1}[z^{-k}\mathbf{B}(\bar{\mathbf{q}}_s')^{-1}(\mathbf{V}\bar{\mathbf{F}}_s')\mathbf{w}(t) + \mathbf{C}\boldsymbol{\xi}(t)] \tag{18}$$

If we set

$$\bar{\mathbf{F}}_s' = \mathbf{A} \tag{19}$$

then equation (18) becomes after some arrangement:

$$\mathbf{y}(t) = [\mathbf{A} + z^{-k}\mathbf{B}(\bar{\mathbf{q}}_s')^{-1}\mathbf{V}\mathbf{A}]^{-1}(z^{-k}\mathbf{B})(\bar{\mathbf{q}}_s')^{-1}[\mathbf{V}(\mathbf{A})\mathbf{w}(t) + \bar{\mathbf{q}}_s'(z^{-k}\mathbf{B})^{-1}\mathbf{C}\boldsymbol{\xi}(t)] \tag{20}$$

Next, we can introduce the following relation [6]:

$$(\mathbf{A} + z^{-k}\mathbf{B}[\bar{\mathbf{q}}_s']^{-1}\mathbf{V}\mathbf{A})^{-1}z^{-k}\mathbf{B}(\bar{\mathbf{q}}_s')^{-1} = \mathbf{A}^{-1}z^{-k}\mathbf{B}(\bar{\mathbf{q}}_s' + z^{-k}\mathbf{V}\mathbf{B})^{-1} \tag{21}$$

Making use of equations (20) and (21), we obtain:

$$\mathbf{y}(t) = \mathbf{A}^{-1}z^{-k}\mathbf{B}(\bar{\mathbf{q}}_s' + z^{-k}\mathbf{V}\mathbf{B})^{-1}[\mathbf{V}(\mathbf{A})\mathbf{w}(t) + \bar{\mathbf{q}}_s'(z^{-k}\mathbf{B})^{-1}\mathbf{C}\boldsymbol{\xi}(t)] \tag{22}$$

The desired closed loop configuration is achieved by setting:

$$(\bar{\mathbf{q}}'_s + z^{-k}\mathbf{VB}) = \mathbf{CT}'\mathbf{K}' \tag{23}$$

where $\mathbf{T}'$ represents the desired closed loop poles.
It is assumed, without loss of generality, that $\mathbf{T}'$ is normalised such that

$$\mathbf{T}'(1) = \mathbf{I} \tag{24}$$

The above equation can easily be satisfied by selecting $\mathbf{T}'$ such that [6]:

$$\mathbf{T}'(z^{-1}) = (\mathbf{I} + \mathbf{T}'_1 + \ldots, \ldots + \mathbf{T}'_{n_{T'}})^{-1}(\mathbf{I} + \mathbf{T}'_1 z^{-1} + \mathbf{T}_2 z^{-2} + \ldots.., \ldots.. + \mathbf{T}'_{n_{T'}} z^{n_{T'}}) \tag{25}$$

Here $\mathbf{K}'$ is ($n \times n$) user-defined gain matrix that has to be chosen such that the steady state error is zero. It can be seen from (17) and (23) that the user-defined gain matrix $\mathbf{K}'$ is employed to ensure the incorporation of the integral action into the design (i.e. $\bar{\mathbf{q}}'_s(1)$ in equation (23) equal to zero).
where $n_{T'}$ represents the degree of the polynomials $\mathbf{T}'$.
Using equations (19) and (23) and rearranging, we obtain:

$$\bar{\mathbf{q}}'_s = \mathbf{CT}'\mathbf{K}' - z^{-k}\mathbf{VB} \tag{26}$$

It can be seen from (17) and (26) that in order to ensure that $\bar{\mathbf{q}}'_s$ involves ($\Delta$)(i.e. $\bar{\mathbf{q}}'_s(1)$ in equation (23) equal to zero), we set:

$$\bar{\mathbf{q}}'_s(1) = \mathbf{C}(1)\mathbf{T}'(1)\mathbf{K}' - \mathbf{VB}(1) = 0 \tag{27}$$

The above equation (27) can be satisfied by setting:

$$\mathbf{K}' = [\mathbf{C}(1)\mathbf{T}'(1)]^{-1}(\mathbf{VB}(1)) = [\mathbf{C}(1)]^{-1}\mathbf{VB}(1) \tag{28}$$

We can easily compute $\bar{\mathbf{Q}}'_s$ from equation (17) as follows:

$$\left.\begin{aligned} \bar{\mathbf{Q}}'_{s_0} &= \bar{\mathbf{q}}'_{s_0} \\ \bar{\mathbf{Q}}'_{s_i} &= \sum_{j=0}^{i} \bar{\mathbf{q}}'_{s_i} \end{aligned}\right\} \tag{29}$$

If we assume that the degree of $\bar{\mathbf{F}}'_s(z^{-1})$ is equal to 2, then equation (16) becomes:

$$\Delta\bar{\mathbf{Q}}'_s\mathbf{u}(t) = [\mathbf{V}(\bar{\mathbf{F}}'_{s0} + \bar{\mathbf{F}}'_{s1} z^{-1} + \bar{\mathbf{F}}'_{s2} z^{-2})[\mathbf{w}(t) - \mathbf{y}(t)] \tag{30}$$

However, the zeros may be used to achieve better set point tracking or they may also help reduce the magnitude of the control action [5, 7, 11]. In the following section (2.3) a new implicit zero pole-placement is derived.

### 2.3 New Implicit Multivariable PID Zero Pole-placement Controller (Mode 3)

If we set the desired closed loop zeros matrix $\tilde{\mathbf{H}}' \neq \mathbf{I}$ , then the control law given by equation (9) can be expressed as follows:

$$\bar{\mathbf{q}}_s'\mathbf{u}(t) = [\mathbf{V}\bar{\mathbf{F}}_s'\mathbf{w}(t) - \tilde{\mathbf{H}}'\mathbf{V}\bar{\mathbf{F}}_s'\mathbf{y}(t)] \tag{31}$$

By combining equations (31) and (1), the closed loop transfer function is obtained as:

$$\mathbf{y}(t) = (\mathbf{A} + z^{-k}\mathbf{B}[\bar{\mathbf{q}}_s']^{-1}\tilde{\mathbf{H}}'\mathbf{V}\bar{\mathbf{F}}_s')^{-1}[z^{-k}\mathbf{B}(\bar{\mathbf{q}}_s')^{-1}(\tilde{\mathbf{H}}'\mathbf{V}\bar{\mathbf{F}}_s')\mathbf{w}(t) + \mathbf{C}\boldsymbol{\xi}(t)] \tag{32}$$

If we assume, without loss of generality, at steady state that:

$$\left.\begin{aligned} \bar{\mathbf{F}}_s' &= \mathbf{A}\mathbf{K}_0 \\ \mathbf{H}_s' &= \tilde{\mathbf{H}}'\,\mathbf{V} \end{aligned}\right\} \tag{33}$$

then equation (32) becomes after some arrangement:

$$\begin{aligned} \mathbf{y}(t) = [\mathbf{A} + z^{-k}\mathbf{B}(\bar{\mathbf{q}}_s')^{-1}\tilde{\mathbf{H}}_s'\mathbf{A}]^{-1}(z^{-k}\mathbf{B})(\bar{\mathbf{q}}_s')^{-1}[(\tilde{\mathbf{H}}_s'\mathbf{A}(1)\mathbf{K}_0)\mathbf{w}(t) + \\ \bar{\mathbf{q}}_s'(z^{-k}\mathbf{B})^{-1}\mathbf{C}\boldsymbol{\xi}(t)] \end{aligned} \tag{34}$$

Next, we can introduce the following relation [5]:

$$(\mathbf{A} + z^{-k}\mathbf{B}[\bar{\mathbf{q}}_s']^{-1}\tilde{\mathbf{H}}_s'\mathbf{A})^{-1}z^{-k}\mathbf{B}(\bar{\mathbf{q}}_s')^{-1} = \mathbf{A}^{-1}z^{-k}\mathbf{B}(\bar{\mathbf{q}}_s' + z^{-k}\tilde{\mathbf{H}}_s'\mathbf{B})^{-1} \tag{35}$$

Making use of equations (35) and (34), we obtain:

$$\mathbf{y}(t) = \mathbf{A}^{-1}z^{-k}\mathbf{B}(\bar{\mathbf{q}}_s' + z^{-k}\tilde{\mathbf{H}}_s'\mathbf{B})^{-1}[(\tilde{\mathbf{H}}_s'\mathbf{A}\mathbf{K}_0)\mathbf{w}(t) + \bar{\mathbf{q}}_s'(z^{-k}\mathbf{B})^{-1}\mathbf{C}\boldsymbol{\xi}(t)] \tag{36}$$

The desired closed loop configuration is achieved by setting:

$$(\bar{\mathbf{q}}_s' + z^{-k}\tilde{\mathbf{H}}_s'\mathbf{B}) = \mathbf{C}\mathbf{T}'\mathbf{K}' \tag{37}$$

where $\mathbf{T}'$ represents the desired closed loop poles and $\tilde{\mathbf{H}}'$ represents the desired closed loop zeros.

It is assumed, without loss of generality, that $\mathbf{T}'$ and $\tilde{\mathbf{H}}'$ are normalised such that

$$\mathbf{T}'(1) = \tilde{\mathbf{H}}'(1) \tag{38}$$

The above equation can easily be satisfied by selecting $\mathbf{T}'$ and $\tilde{\mathbf{H}}'$ such that [5]:

$$\tilde{\mathbf{H}}'(z^{-1}) = (\mathbf{I} + \tilde{\mathbf{h}}' + .... + \tilde{\mathbf{h}}_{n_{\tilde{h}'}})^{-1}(\mathbf{I} + \tilde{\mathbf{h}}_1' z^{-1} + ...... + \tilde{\mathbf{h}}_{n_{\tilde{h}'}} z^{-n_{\tilde{h}'}}) \tag{39}$$

$$\mathbf{T}'(z^{-1}) = (\mathbf{I} + \mathbf{T}_1' + ...,... + \mathbf{T}_{n_{T'}}')^{-1}(\mathbf{I} + \mathbf{T}_1' z^{-1} + \mathbf{T}_2 z^{-2} + .....,..... + \mathbf{T}_{n_{T'}}' z^{n_{T'}}) \tag{40}$$

Here $\mathbf{K}'$ is the ($n \times n$) user-defined gain matrix that has to be chosen such that the steady state error is zero. It can be seen from (17) and (37) that the user-defined gain matrix $\mathbf{K}'$ is employed to ensure the incorporation of the integral action into the design (i.e. $\bar{\mathbf{q}}_s'(1)$ in equation (37) equal to zero) [5].
where $n_{T'}$ and $n_{\tilde{h}'}$ represents the degree of the polynomials $\mathbf{T}'$ and $\tilde{\mathbf{H}}'$, respectively.
Using equations(33) and (37) and rearranging, we obtain:

$$\bar{\mathbf{q}}_s' = \mathbf{C}\mathbf{T}'\mathbf{K}' - z^{-k}\tilde{\mathbf{H}}'\mathbf{V}\mathbf{B} \tag{41}$$

It can be seen from (17) and (41) that in order to ensure that $\bar{\mathbf{q}}_s'$ involves ($\Delta$)(i.e. $\bar{\mathbf{q}}_s'(1)$ in equation (37) equal to zero), we set:

$$\bar{\mathbf{q}}_s'(1) = \mathbf{C}(1)\mathbf{T}'(1)\mathbf{K}' - \tilde{\mathbf{H}}'(1)\mathbf{V}\mathbf{B}(1) = 0 \tag{42}$$

The above equation (42) can be satisfied by setting:

$$\mathbf{K}' = [\mathbf{C}(1)\mathbf{T}'(1)]^{-1}(\tilde{\mathbf{H}}'(1)\mathbf{V}\mathbf{B}(1)) = [\mathbf{C}(1)]^{-1}\mathbf{V}\mathbf{B}(1) \tag{43}$$

It can be seen from equation (36) that the closed loop poles will be placed in the desired locations if we assume the following:

$$\left.\begin{aligned} \mathbf{X}_s &= \tilde{\mathbf{H}}_s'\mathbf{A} \\ \mathbf{K}_0 &= \mathbf{K}_0'[\mathbf{K}_0'(1)]^{-1} \\ \tilde{\mathbf{K}}_0'\tilde{\mathbf{X}}_s &= \mathbf{X}_s\mathbf{K}_0' \\ \tilde{\mathbf{K}}_0' &= \mathbf{C} \end{aligned}\right\} \tag{44}$$

The new implicit multivariable pole-zero placement controller block diagram is shown in Figure (1a).
The implicit pole-zero placement controller illustrated in Figure (1a) is now extended to combine the advantages of both PID control and pole-zero placement control. In order to show the inherent incorporation of the PID control explicitly in our design, the polynomial $\bar{\mathbf{q}}_s'$ in equation (17) must be split into an integral action ($\Delta$) part and a pole-placement compensator $\bar{\mathbf{Q}}_s'$.

We can easily compute $\bar{\mathbf{q}}'_s$ from equation (17) as follows:

$$\left.\begin{aligned} \bar{\mathbf{Q}}'_{s_0} &= \bar{\mathbf{q}}'_{s_0} \\ \bar{\mathbf{Q}}'_{s_i} &= \sum_{j=0}^{i} \bar{\mathbf{q}}'_{s_i} \end{aligned}\right\} \tag{45}$$

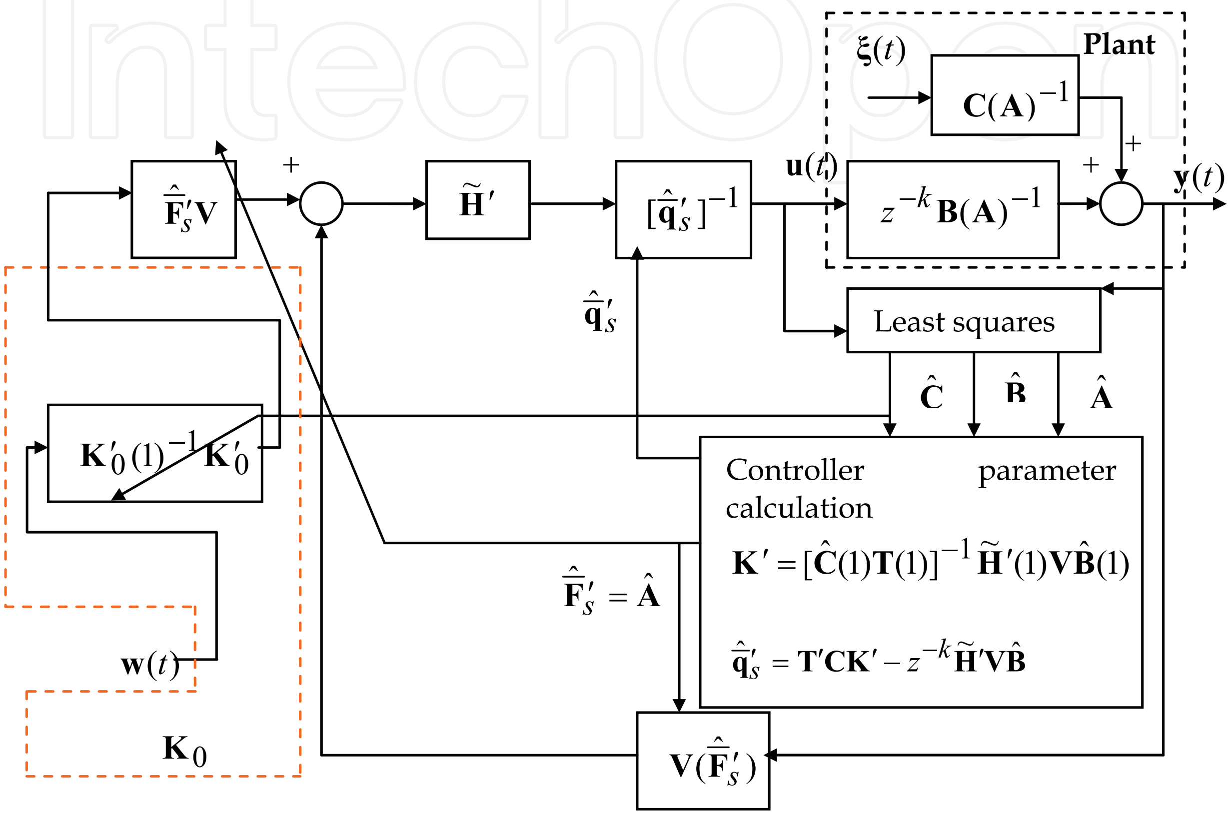


Fig. (1a). New implicit multivariable pole-zero placement controller.

If we assume that the degree of $\bar{\mathbf{F}}'_s(z^{-1})$ is equal to 2, then equation (31) becomes:

$$\begin{aligned} \Delta\bar{\mathbf{Q}}'_s\mathbf{u}(t) = \tilde{\mathbf{H}}[&\mathbf{V}(\bar{\mathbf{F}}'_{s0} + \bar{\mathbf{F}}'_{s1}z^{-1} + \bar{\mathbf{F}}'_{s2}z^{-2})\mathbf{K}_0\mathbf{w}(t) - \\ &\mathbf{V}(\bar{\mathbf{F}}'_{s0} + \bar{\mathbf{F}}'_{s1}z^{-1} + \bar{\mathbf{F}}'_{s2}z^{-2})\mathbf{y}(t)] \end{aligned} \tag{46}$$

The controller parameters $\mathbf{K}_0$, $\bar{\mathbf{Q}}'_s$ and $\bar{\mathbf{F}}'_s(z^{-1})$ in the above equation (46) are obtained from the equations (44), (46) and (33) respectively.
The implicit pole-zero placement control law given by equation (46) is shown in Figure (1b). It can be seen from the above equation (46) and Figure (1b) that the pole-zero placement controller can be represented by an equivalent controller consisting of a PID controller plus three compensators labelled as compensator 1, compensator 2 and compensator 3 in the Figure (1b). The first compensator is used to ensure that at steady state, the output signal tracks the set point. The compensator 2 is used to achieve pole-placement control and compensator 3 is used to achieve zero-placement.

From equation (33) it is clear that a PI controller is achieved if the polynomial $\mathbf{A}(z^{-1})$ is of order 1, whereas, a PID controller is achieved if $\mathbf{A}(z^{-1})$ is of order 2.
A pure PI/PID control is achieved if these three compensators are switched off.
The algorithm for the pole-zero placement controller can then be summarised as follows:
Step 1. Select the desired closed-loop system poles and zeros polynomial matrices, $\mathbf{T}'(z^{-1})$ and $\tilde{\mathbf{H}}'(z^{-1})$ respectively, and select the user-defined gain matrix $\mathbf{V}$.
Step 2. Read the new values of the output $\mathbf{y}(t)$, the control input $\mathbf{u}(t)$ and reference signal $\mathbf{w}(t)$
Step 3. Estimate the process parameters $\hat{\mathbf{A}}$, $\hat{\mathbf{B}}$, and $\hat{\mathbf{C}}$ using the linear least squares algorithm.
Step 4. Set $\overline{\mathbf{F}}_s'(z^{-1}) = \hat{\mathbf{A}}(z^{-1})$.
Step 5. Compute $\mathbf{K}_0$ and $\mathbf{K}'$ using equations (44) and (43), respectively.
Step 6. Compute $\hat{\overline{\mathbf{q}}}_s'$ using equation (41).
Step 7. Apply the control law using equation (31).
Steps 2 to 7 are repeated for every sampling instant.

## 3 Simulation results

The objective of this section is to study the performance and the robustness of the proposed multivariable pole-zero placement controller.
Two simulation examples are carried out in order to demonstrate the ability of the proposed algorithm to locate the closed loop poles and zeros at their pre-specified locations under set point changes. The simulation study also includes an investigation of the influence of the load disturbances and stochastic disturbances on the system. In all performed simulations the least squares estimator has been employed and 800 samples are used with a set point change every 100 sampling instants.
In order to demonstrate the closed loop performance of the implicit controller we arrange manually (for reason of comparison) the controller to work in three control modes, namely as a PID pole-placement controller, a PID pole-zero placement controller and as a PID self-tuning controller as described below:
a) From 0th up to 250th sampling time, the implicit PID pole-placement controller is selected to operate on-line.
b) The Implicit PID pole-zero placement controller is switched on from 251st to 550th sampling times.
c) The conventional PID self-tuning controller is switched on from 551st to 800th sampling time.
Two case studies are considered in this section: a two-input two-output water bath system and a simulated non-minimum phase system.

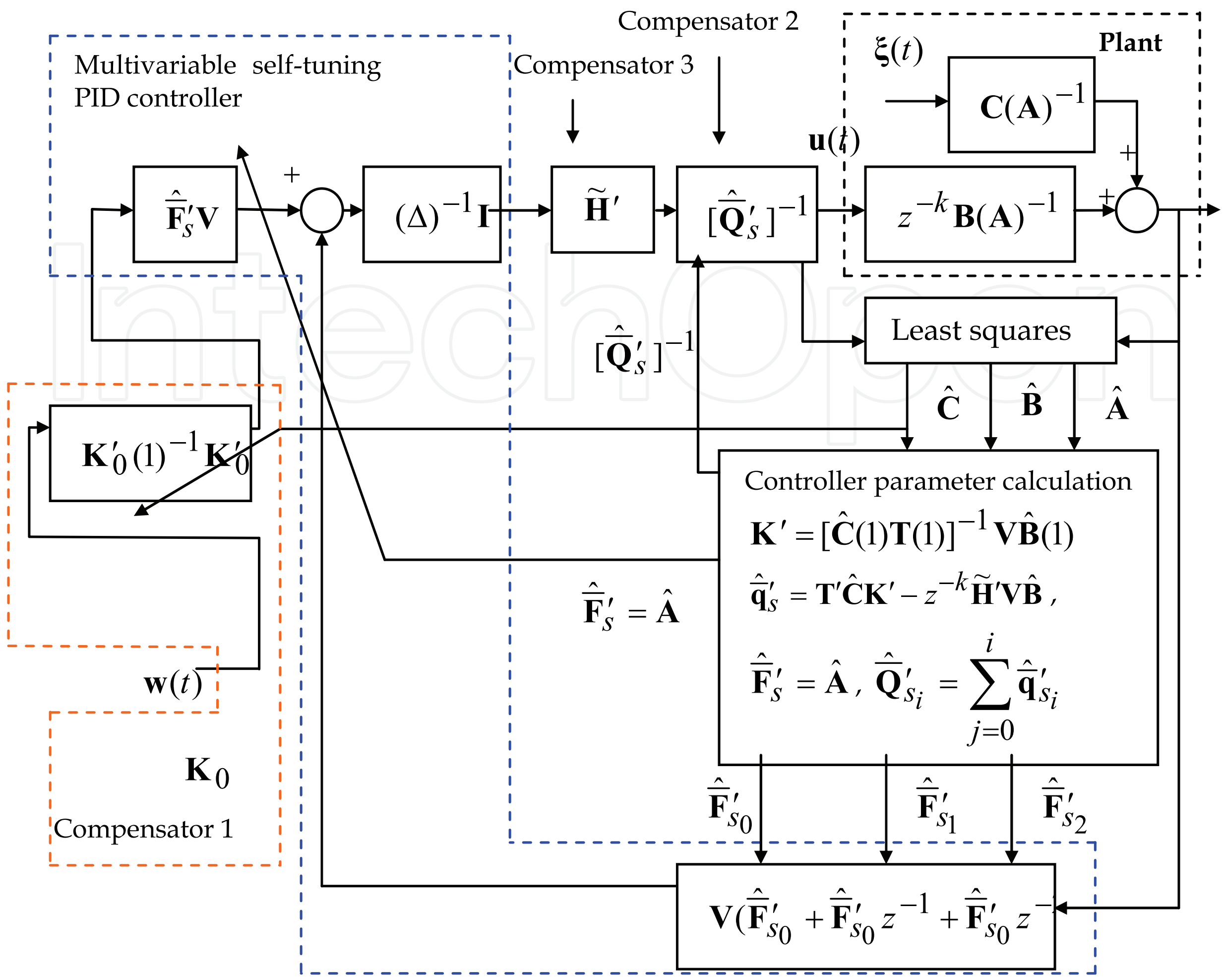


Fig. (1b). Novel implicit multivariable PID pole-zero placement controller.

### 3.1 Case study 1: Two-input Two-output Water Bath System Simulation results

The algorithm proposed in sections (2.2) was applied to a two-input two-output water bath treated previously by Yusof et al. [2, 13] and Zayed et al. [4, 10, 11]. The water bath system is shown in Figure (2). The water bath is an example of an important component in many industrial chemical processes. The control objective is to bring the temperature of the water or some chemical product in the bath to the desired set-points as accurately as possible. The discrete model of the water bath system can be written as [2, 10, 11]:

$$(\mathbf{I}+\mathbf{A}_1 z^{-1})\mathbf{y}(t)=\mathbf{B}_0\mathbf{u}(t-k)+\xi(t) \tag{47}$$

where

$$\mathbf{A}_1=\begin{bmatrix}-0.411 & -0.634\\ -0.103 & -0.885\end{bmatrix},\ \mathbf{B}_0=\begin{bmatrix}0.492 & 0.085\\ 0.041 & 0.237\end{bmatrix}$$

and the sample time = 30 sec.

The simulation was performed over 800 samples (400 minutes) under set point $\mathbf{w}(t)=\begin{bmatrix}\mathbf{w}_1(t)\\ \mathbf{w}_2(t)\end{bmatrix}$ changes every 100 sampling instants as follows:

1) $\mathbf{w}_1(t)$ changes from $60^0\mathrm{C}$ to $80^0\mathrm{C}$ and from $80^0\mathrm{C}$ to $60^0\mathrm{C}$.

2) $\mathbf{w}_2(t)$ changes from $35^0\mathrm{C}$ to $55^0\mathrm{C}$ and from $55^0\mathrm{C}$ to $35^0\mathrm{C}$.

In each sampling instant the parameter estimations $\hat{\mathbf{A}}_1$ and $\hat{\mathbf{B}}_0$ are estimated using the least squares estimator and the steps summarised in section (2) are followed.
Note that, by selecting the pre-filter polynomial matrix $\mathbf{P}_d(z^{-1})$ to be of order one, a PI self-tuning controller is obtained.
The user-defined gain and the pre-filter polynomial matrices were respectively selected as:

$$\mathbf{V} = \begin{bmatrix} \mathrm{V}_1 & 0 \\ 0 & \mathrm{V}_2 \end{bmatrix} = \begin{bmatrix} 0.7 & 0 \\ 0 & 0.8 \end{bmatrix},\ \mathbf{P}_d(z^{-1}) = \mathbf{I} + \mathbf{P}_{d_1} z^{-1} \text{ and } \mathbf{P}_n(z^{-1}) = \mathbf{I} + \mathbf{P}_{n_1} z^{-1}.$$

where,

$$\mathbf{P}_{d_1}(z^{-1}) = \begin{bmatrix} -0.8 & 0 \\ 0 & -0.9 \end{bmatrix} \text{ and } \mathbf{P}_{n_1}(z^{-1}) = \begin{bmatrix} -0.3 & 0 \\ 0 & -0.4 \end{bmatrix}.$$

The desired closed loop poles polynomial matrix ($\mathbf{T}$) and the desired zero-placement polynomial matrix ($\tilde{\mathbf{H}}$) were selected as follows:

$$\left.\begin{aligned} \mathbf{T}(z^{-1}) &= \mathbf{I} + \mathbf{T}_1 z^{-1} + \mathbf{T}_2 z^{-2} \\ \tilde{\mathbf{H}}(z^{-1}) &= [\tilde{\mathbf{h}}(1)]^{-1}(\mathbf{I} + \tilde{\mathbf{h}}_1 z^{-1} + \tilde{\mathbf{h}}_2) z^{-2} \end{aligned}\right\}$$

where

$$\mathbf{T}_1 = \begin{bmatrix} -0.5 & 0 \\ 0 & -0.6 \end{bmatrix},\ \mathbf{T}_2 = \begin{bmatrix} 0 & 0 \\ 0 & 0 \end{bmatrix},\ \tilde{\mathbf{h}}_1 = \begin{bmatrix} 0.9 & 0 \\ 0 & 0.8 \end{bmatrix} \text{ and } \tilde{\mathbf{h}}_2 = \begin{bmatrix} 0 & 0 \\ 0 & 0 \end{bmatrix}.$$

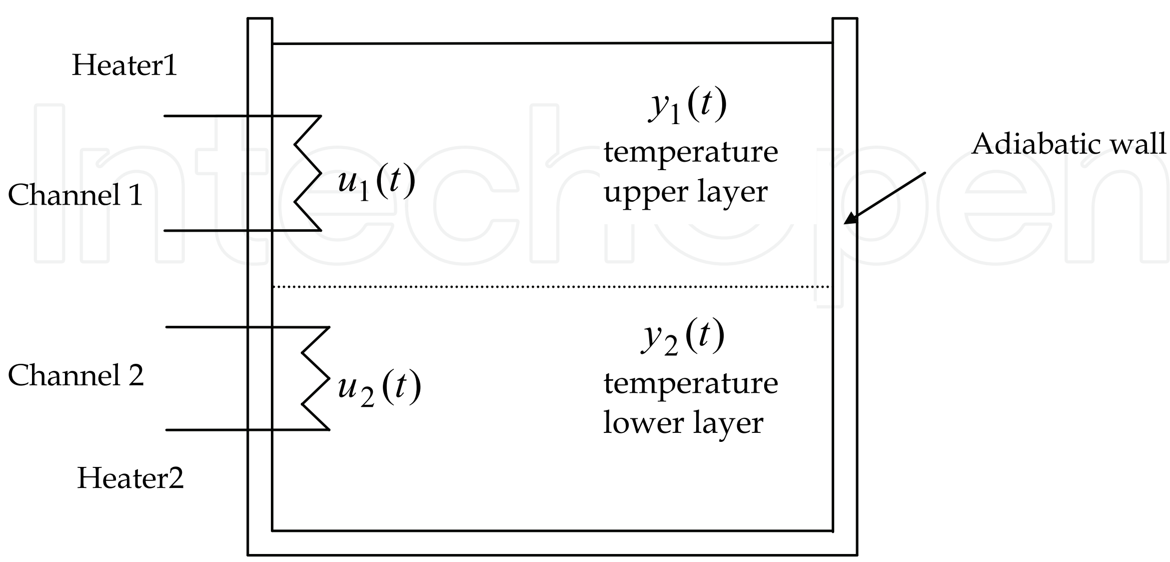


Fig. (2). A two channel water bath system

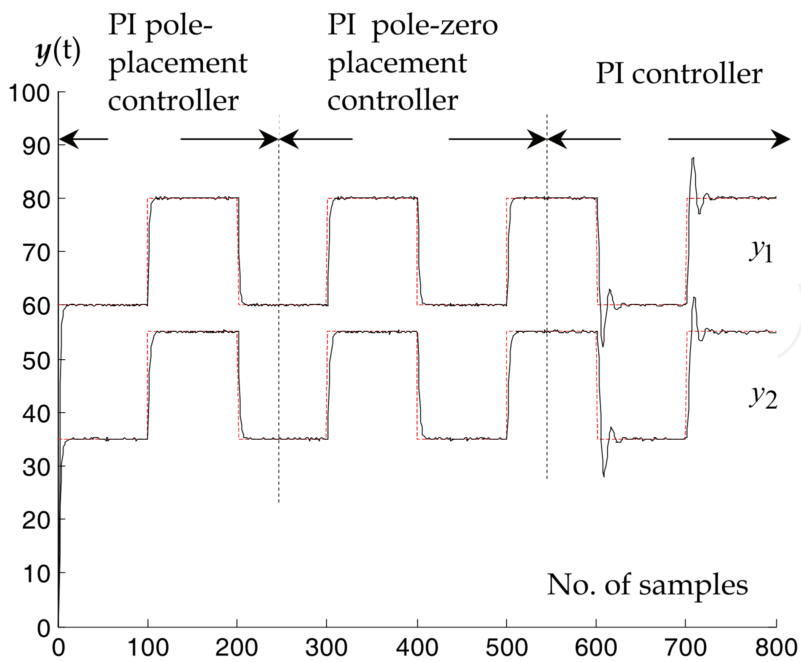


$$\mathbf{V} = \begin{bmatrix} 0.7 & 0 \\ 0 & 0.8 \end{bmatrix}, \quad \mathbf{P}_{n_1} = \begin{bmatrix} -0.3 & 0 \\ 0 & -0.4 \end{bmatrix}, \quad \mathbf{P}_{d_1} = \begin{bmatrix} -0.8 & 0 \\ 0 & -0.9 \end{bmatrix}, \quad \mathbf{T}_1 = \begin{bmatrix} -0.5 & 0 \\ 0 & -0.6 \end{bmatrix}$$

and $\mathbf{T}_2 = \begin{bmatrix} 0 & 0 \\ 0 & 0 \end{bmatrix}$. $\tilde{\mathbf{h}}_1 = \begin{bmatrix} 0.9 & 0 \\ 0 & 0.8 \end{bmatrix}$ and $\tilde{\mathbf{h}}_2 = \begin{bmatrix} 0 & 0 \\ 0 & 0 \end{bmatrix}$.

Fig. (3a). The outputs

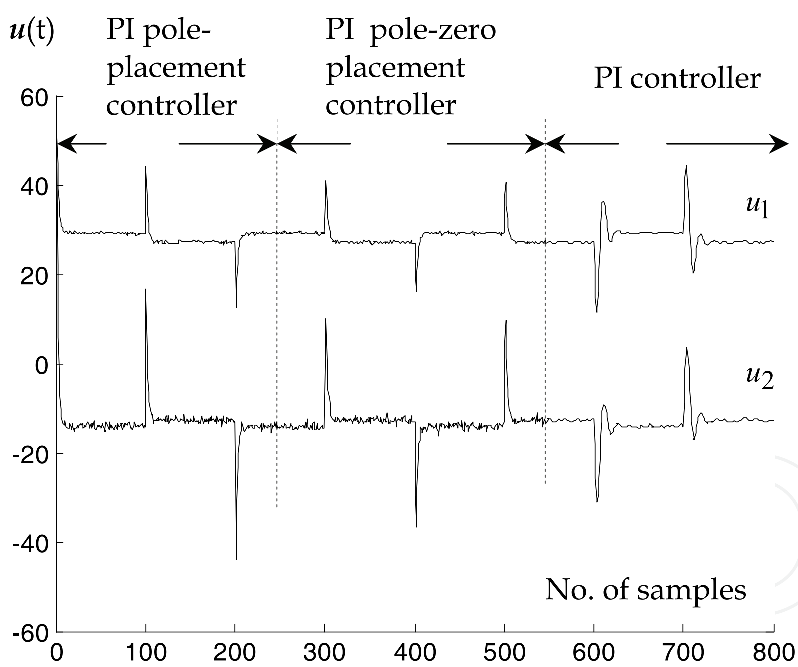


$$\mathbf{V} = \begin{bmatrix} 0.7 & 0 \\ 0 & 0.8 \end{bmatrix}, \quad \mathbf{P}_{n_1} = \begin{bmatrix} -0.3 & 0 \\ 0 & -0.4 \end{bmatrix}, \quad \mathbf{P}_{d_1} = \begin{bmatrix} -0.8 & 0 \\ 0 & -0.9 \end{bmatrix}, \quad \mathbf{T}_1 = \begin{bmatrix} -0.5 & 0 \\ 0 & -0.6 \end{bmatrix}$$

and $\mathbf{T}_2 = \begin{bmatrix} 0 & 0 \\ 0 & 0 \end{bmatrix}$. $\tilde{\mathbf{h}}_1 = \begin{bmatrix} 0.9 & 0 \\ 0 & 0.8 \end{bmatrix}$ and $\tilde{\mathbf{h}}_2 = \begin{bmatrix} 0 & 0 \\ 0 & 0 \end{bmatrix}$.

Fig. (3b). The control inputs

The outputs and the control inputs of the multiple controller are respectively shown in the Figures (3a) and (3b).

It is clear from these Figures (3a) and (3b) that, the transient response is significantly shaped by the choice of the polynomial $\mathbf{T}$ when either a PI pole-placement controller or a PI pole-zero placement controller is used. It can also clearly be seen from Figure (3b) that excessive control action, which resulted from set-point changes, is tuned most effectively when the new implicit PI zero-pole placement controller is on-line (during the sampling interval

251-550). Also note that during the last 250 samples (551-800 sampling times), where the conventional self tuning PI is operating, small oscillations can be seen in the control input and closed loop output, hence exhibiting the worst performance as expected, due to its inherent limitations. The other disadvantage of the self-tuning PID controller is that the tuning parameters must be selected using a trial and error procedure. The performance of the conventional PI controller can be improved by fine adjusting the user defined polynomial matrices $\mathbf{P}_n(z^{-1})$, $\mathbf{P}_d(z^{-1})$ and gain matrix $\mathbf{V}$.

The following simulation experiment investigates the effect of the user-defined parameter **V** on the response of the closed loop system when the PI multiple-controller is used.

#### 3.1.1 Investigating the Influence of the Gain $\mathbf{V}$ on the Closed-Loop Performance

In order to see the effect of the user-defined gain on all controllers (the PI controller, PI pole-placement controller and PI pole-zero placement controller), the gain matrix **V** was changed from $\mathbf{V}=\begin{bmatrix}0.7 & 0\\ 0 & 0.8\end{bmatrix}$ to $\mathbf{V}=\begin{bmatrix}2 & 0\\ 0 & 0.8\end{bmatrix}$ (only $\mathrm{V}_1$ was increased). The outputs and the control inputs are respectively shown in the Figures (4a) and (4b).

It is clear from these Figures (4a) and (4b) that increasing only the gain $V_1$ influences the outputs $y_1(t)$ and $y_2(t)$, when the PI controller is used, whereas the desired outputs are obtained (as expected) when the implicit PI pole-placement or the implicit PI pole-zero placement controllers is turned on. It can clearly be seen from Figure (4a) that the control action $u_1$ is increased.

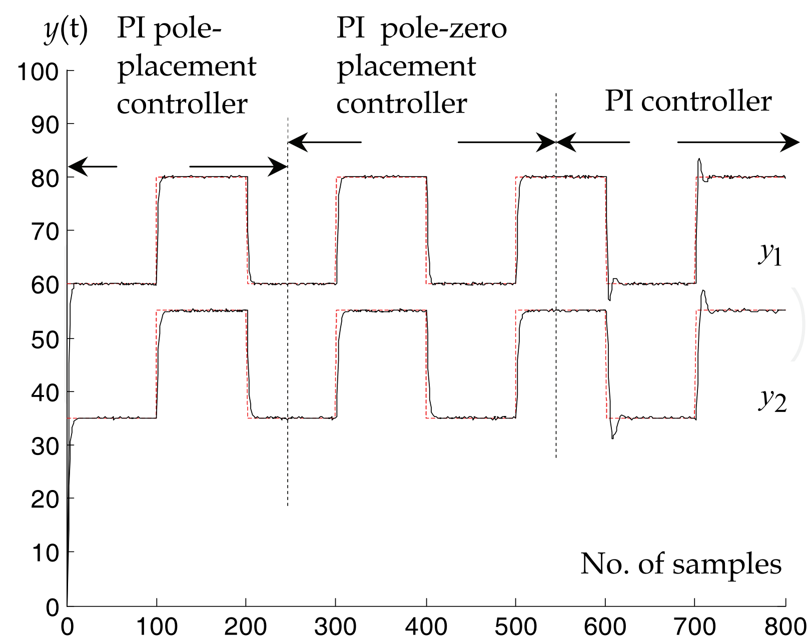


$\mathbf{V}=\begin{bmatrix}2 & 0\\ 0 & 0.8\end{bmatrix}$, $\mathbf{P}_{n_1}=\begin{bmatrix}-0.3 & 0\\ 0 & -0.4\end{bmatrix}$, $\mathbf{P}_{d_1}=\begin{bmatrix}-0.8 & 0\\ 0 & -0.9\end{bmatrix}$, $\mathbf{T}_1=\begin{bmatrix}-0.5 & 0\\ 0 & -0.6\end{bmatrix}$ and $\mathbf{T}_2=\begin{bmatrix}0 & 0\\ 0 & 0\end{bmatrix}$. $\tilde{\mathbf{h}}_1=\begin{bmatrix}0.9 & 0\\ 0 & 0.8\end{bmatrix}$ and $\tilde{\mathbf{h}}_2=\begin{bmatrix}0 & 0\\ 0 & 0\end{bmatrix}$.

Fig. (4a). The outputs

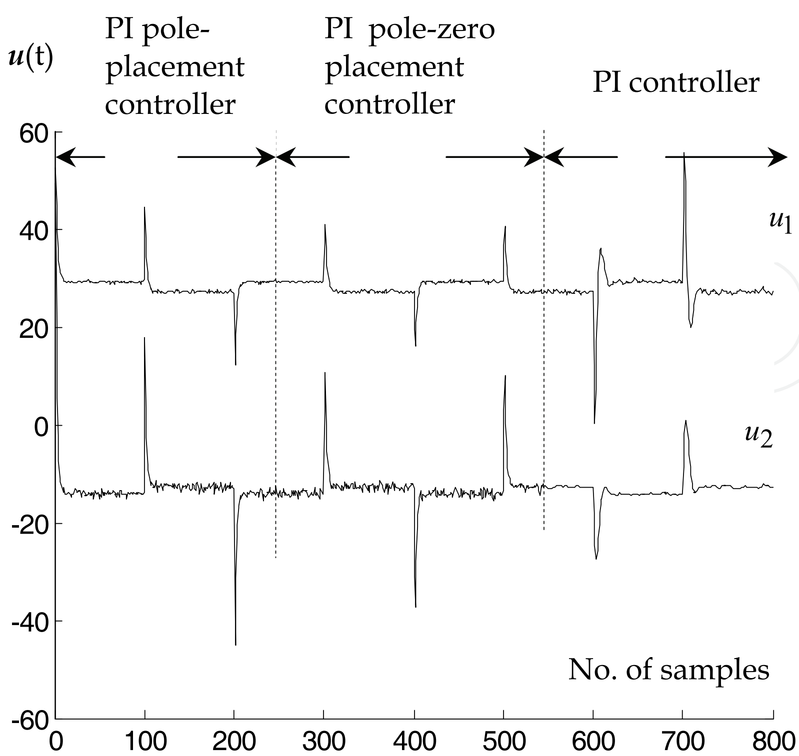


$$\mathbf{V}=\begin{bmatrix}2 & 0\\ 0 & 0.8\end{bmatrix},\ \mathbf{P}_{n_1}=\begin{bmatrix}-0.3 & 0\\ 0 & -0.4\end{bmatrix},\ \mathbf{P}_{d_1}=\begin{bmatrix}-0.8 & 0\\ 0 & -0.9\end{bmatrix},\ \mathbf{T}_1=\begin{bmatrix}-0.5 & 0\\ 0 & -0.6\end{bmatrix}\ \text{and}\ \mathbf{T}_2=\begin{bmatrix}0 & 0\\ 0 & 0\end{bmatrix}.\ \tilde{\mathbf{h}}_1=\begin{bmatrix}0.9 & 0\\ 0 & 0.8\end{bmatrix}\ \text{and}\ \tilde{\mathbf{h}}_2=\begin{bmatrix}0 & 0\\ 0 & 0\end{bmatrix}.$$

Fig. (4b). The control inputs

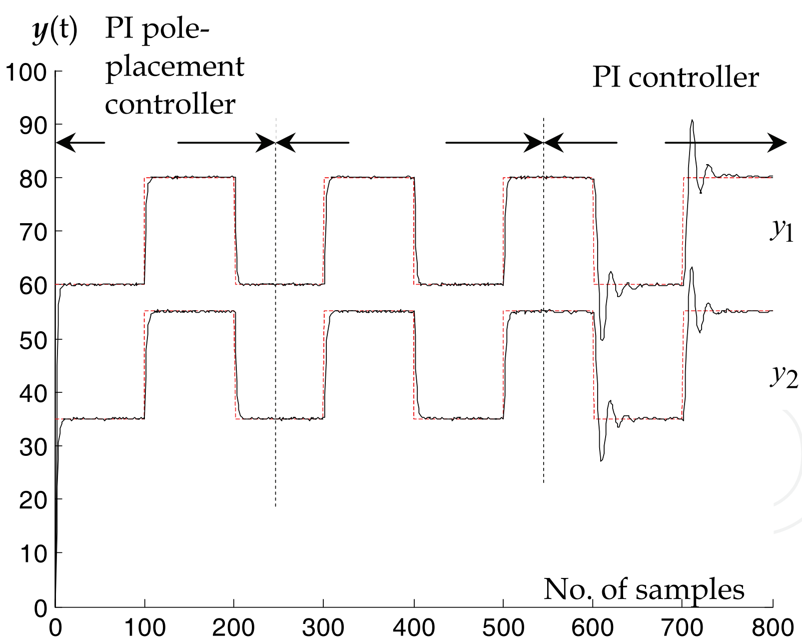


$$\mathbf{V}=\begin{bmatrix}0.1 & 0\\ 0 & 0.8\end{bmatrix},\ \mathbf{P}_{n_1}=\begin{bmatrix}-0.3 & 0\\ 0 & -0.4\end{bmatrix},\ \mathbf{P}_{d_1}=\begin{bmatrix}-0.8 & 0\\ 0 & -0.9\end{bmatrix},\ \mathbf{T}_1=\begin{bmatrix}-0.5 & 0\\ 0 & -0.6\end{bmatrix}\ \text{and}\ \mathbf{T}_2=\begin{bmatrix}0 & 0\\ 0 & 0\end{bmatrix}.\ \tilde{\mathbf{h}}_1=\begin{bmatrix}0.9 & 0\\ 0 & 0.8\end{bmatrix}\ \text{and}\ \tilde{\mathbf{h}}_2=\begin{bmatrix}0 & 0\\ 0 & 0\end{bmatrix}.$$

Fig. (5a). The outputs

The gain $\mathbf{V}$ was again changed from $\mathbf{V}=\begin{bmatrix}2 & 0\\ 0 & 0.8\end{bmatrix}$ to $\mathbf{V}=\begin{bmatrix}0.1 & 0\\ 0 & 0.8\end{bmatrix}$ (only $V_1$ is decreased).

The outputs and the control inputs are respectively shown in the Figures (5a) and (5b).

It can obviously be seen from the above Figures (5a) and (5b) that decreasing only the gain $V_1$ influences the outputs $y_1(t)$ and $y_2(t)$, when the PI controller is used, whereas the demanded outputs are achieved when the PI pole-placement or PI pole-zero placement is turned on.

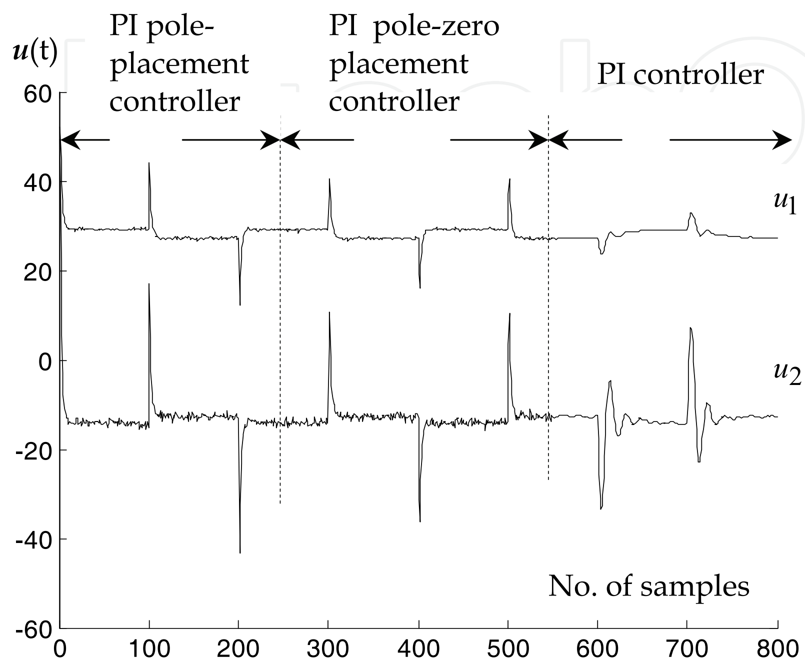


$$\mathbf{V} = \begin{bmatrix} 0.1 & 0 \\ 0 & 0.8 \end{bmatrix}, \ \mathbf{P}_{n_1} = \begin{bmatrix} -0.3 & 0 \\ 0 & -0.4 \end{bmatrix}, \ \mathbf{P}_{d_1} = \begin{bmatrix} -0.8 & 0 \\ 0 & -0.9 \end{bmatrix}, \ \mathbf{T}_1 = \begin{bmatrix} -0.5 & 0 \\ 0 & -0.6 \end{bmatrix}$$

and $\mathbf{T}_2 = \begin{bmatrix} 0 & 0 \\ 0 & 0 \end{bmatrix}$. $\tilde{\mathbf{h}}_1 = \begin{bmatrix} 0.9 & 0 \\ 0 & 0.8 \end{bmatrix}$ and $\tilde{\mathbf{h}}_2 = \begin{bmatrix} 0 & 0 \\ 0 & 0 \end{bmatrix}$.

Fig. (5b). The control inputs

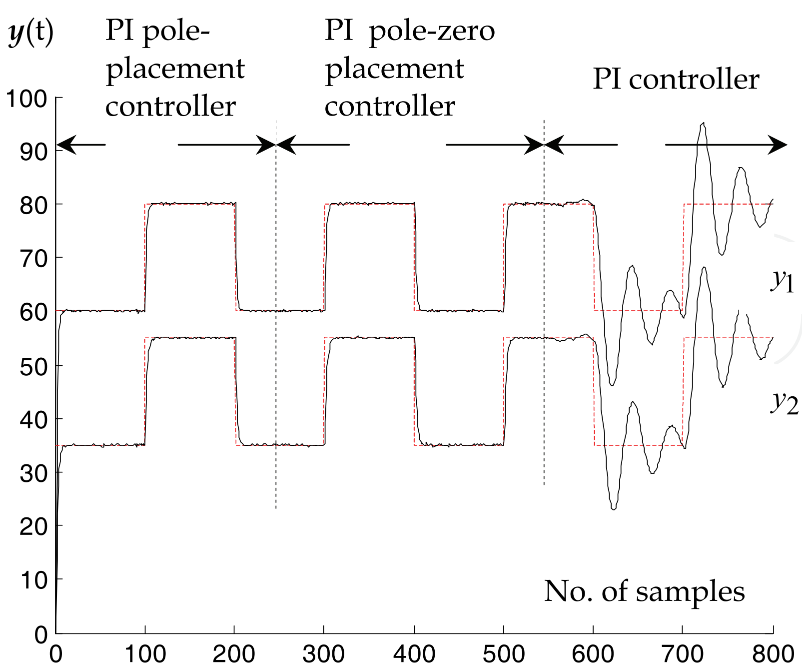


$$\mathbf{V} = \begin{bmatrix} 0.1 & 0 \\ 0 & 0.1 \end{bmatrix}, \ \mathbf{P}_{n_1} = \begin{bmatrix} -0.3 & 0 \\ 0 & -0.4 \end{bmatrix}, \ \mathbf{P}_{d_1} = \begin{bmatrix} -0.8 & 0 \\ 0 & -0.9 \end{bmatrix}, \ \mathbf{T}_1 = \begin{bmatrix} -0.5 & 0 \\ 0 & -0.6 \end{bmatrix}$$

and $\mathbf{T}_2 = \begin{bmatrix} 0 & 0 \\ 0 & 0 \end{bmatrix}$. $\tilde{\mathbf{h}}_1 = \begin{bmatrix} 0.9 & 0 \\ 0 & 0.8 \end{bmatrix}$ and $\tilde{\mathbf{h}}_2 = \begin{bmatrix} 0 & 0 \\ 0 & 0 \end{bmatrix}$.

Fig. (6a). The outputs

The gain **V** was further changed from $\mathbf{V}=\begin{bmatrix}0.1 & 0\\ 0 & 0.8\end{bmatrix}$ to $\mathbf{V}=\begin{bmatrix}0.1 & 0\\ 0 & 0.1\end{bmatrix}$ (only $V_2$ was changed).

The outputs and the control inputs are respectively shown in the Figures (6a) and (6b).
We can clearly see from the Figures (6a) and (6b) that changing the gain $V_2$ affects the outputs $y_1(t)$ and $y_2(t)$ only if the PI controller is used, whereas the desired outputs are obtained when either the implicit PI pole-placement controller or implicit PI pole-zero placement controller is used.

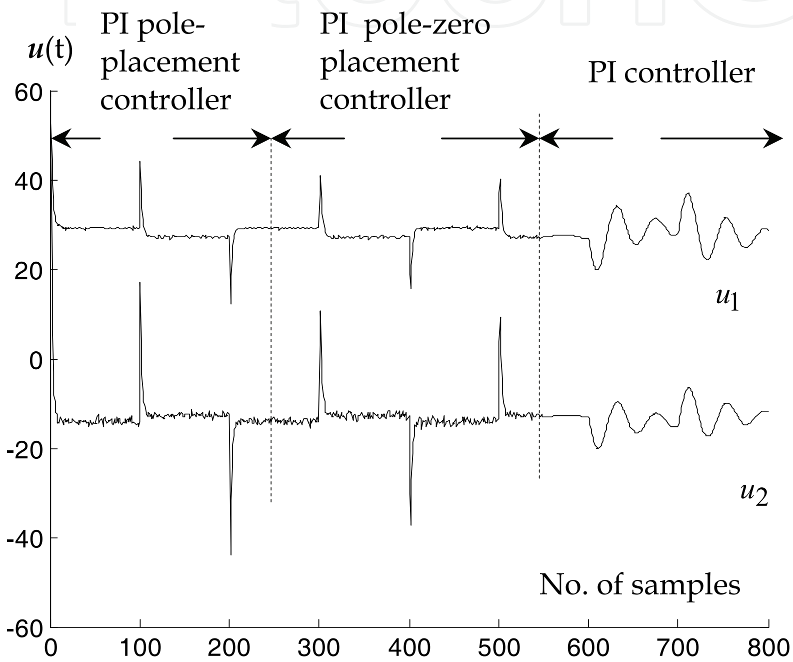


$$\mathbf{V}=\begin{bmatrix}0.1 & 0\\ 0 & 0.1\end{bmatrix},\ \mathbf{P}_{n_1}=\begin{bmatrix}-0.3 & 0\\ 0 & -0.4\end{bmatrix},$$

$$\mathbf{P}_{d_1}=\begin{bmatrix}-0.8 & 0\\ 0 & -0.9\end{bmatrix},$$

$$\mathbf{T}_1=\begin{bmatrix}-0.5 & 0\\ 0 & -0.6\end{bmatrix} \text{ and } \mathbf{T}_2=\begin{bmatrix}0 & 0\\ 0 & 0\end{bmatrix}.$$

$$\tilde{\mathbf{h}}_1=\begin{bmatrix}0.9 & 0\\ 0 & 0.8\end{bmatrix} \text{ and } \tilde{\mathbf{h}}_2=\begin{bmatrix}0 & 0\\ 0 & 0\end{bmatrix}.$$

Fig. (6b). The control inputs

It is clear from the previous figures that changing either $V_1$ or $V_2$ influences the closed loop system responses if the conventional self-tuning PI controller is used.
Excessive changes of either $V_1$ or $V_2$ will produce an unstable closed loop system if the PI self-tuning is used.
The gain matrix **V** has no influence on the closed system if the PI based Pole-zero placement controller is used, since the controller parameters change automatically in response to the change of the gain matrix **V** in order to place the closed loop system poles at pre-specified locations.

### 3.1.2 Investigating the Influence of the load disturbances on the Closed Loop Performance Using implicit Controller

The next task is to see the effect of the load disturbances on the closed system when the implicit PI pole zero placement for MIMO case is used. Artificial load disturbances of values 8°C and 5.5°C (10% of set point values) were added respectively to the outputs $y_1(t)$ and $y_2(t)$, from the 350th sampling interval to 800th sampling interval.

The two controller set points were both kept constant at values of 55°C and 80°C throughout. The outputs and the control inputs for PI pole-zero placement are shown in the Figures (7a) and (7b) respectively.

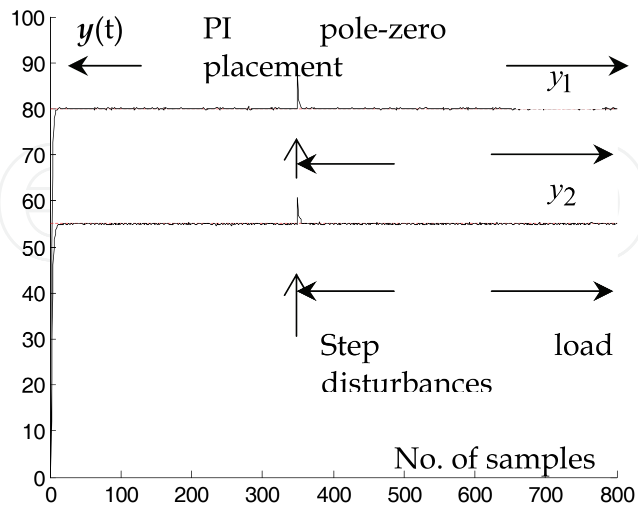


Fig. (7a). The outputs

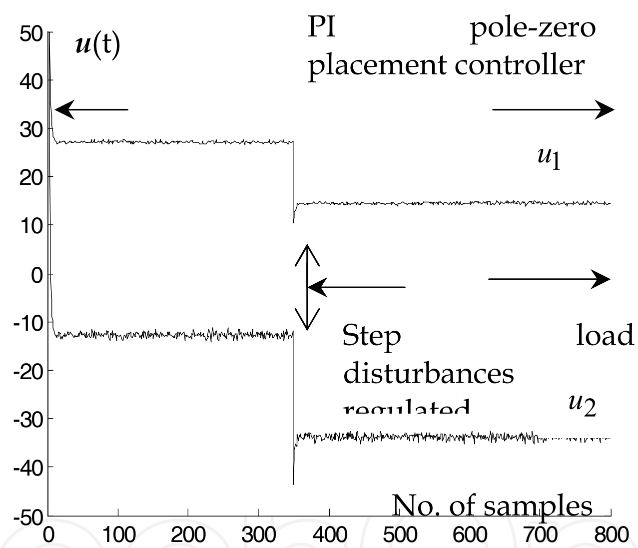


Fig. (7b). The control inputs

It can clearly be seen from all the figures (7a) and (7b) that at steady state, the proposed PI implicit controller has the ability to effectively regulate constant load disturbances to zero.
It can clearly be seen from all the figures (7a) and (7b) that at steady state, the proposed PI implicit controller has the ability to effectively regulate constant load disturbances to zero.

#### 3.1.3 Investigating the Influence of the Polynomial $\tilde{H}$ on the Closed Loop Performance Using Implicit Controller

In order to see the influence of the zeros on the performance of the closed loop system, the implicit PI pole-zero placement was switched on from $t = 0$ up to $t = 800$ and the polynomial matrix $\mathbf{T}$ was fixed as before and only the closed loop zeros polynomial $\tilde{\mathbf{H}}(z^{-1}) = [\tilde{\mathbf{h}}(1)]^{-1}(\mathbf{I} + \tilde{\mathbf{h}}_1 z^{-1} + \tilde{\mathbf{h}}_2 z^{-2})$ was changed three times as follows:

$$
\begin{array}{ll}
0 \le t < 250 & \tilde{\mathbf{h}}(z^{-1}) = \mathbf{I} + \begin{bmatrix} 0.9 & 0 \\ 0 & 0.9 \end{bmatrix} z^{-1} + \begin{bmatrix} 0 & 0 \\ 0 & 0 \end{bmatrix} z^{-2} \\
250 \le t < 550 & \tilde{\mathbf{h}}(z^{-1}) = \mathbf{I} + \begin{bmatrix} -0.7 & 0 \\ 0 & -0.8 \end{bmatrix} z^{-1} + \begin{bmatrix} 0 & 0 \\ 0 & 0 \end{bmatrix} z^{-2} \\
550 \le t < 800 & \tilde{\mathbf{h}}(z^{-1}) = \mathbf{I} + \begin{bmatrix} 0.9 & 0 \\ 0 & 1.4 \end{bmatrix} z^{-1} + \begin{bmatrix} 0.2 & 0 \\ 0 & 0.49 \end{bmatrix} z^{-2}
\end{array} \tag{48}
$$

The outputs and the control inputs are shown in the Figures (8a), (8b) and (8c), respectively. It is clear from the Figures (8a), (8b) and (8c) that changing the polynomial $\tilde{\mathbf{H}}$ affects the closed loop system performance. Excessive control input results from selecting unsuitable $\tilde{\mathbf{H}}$.

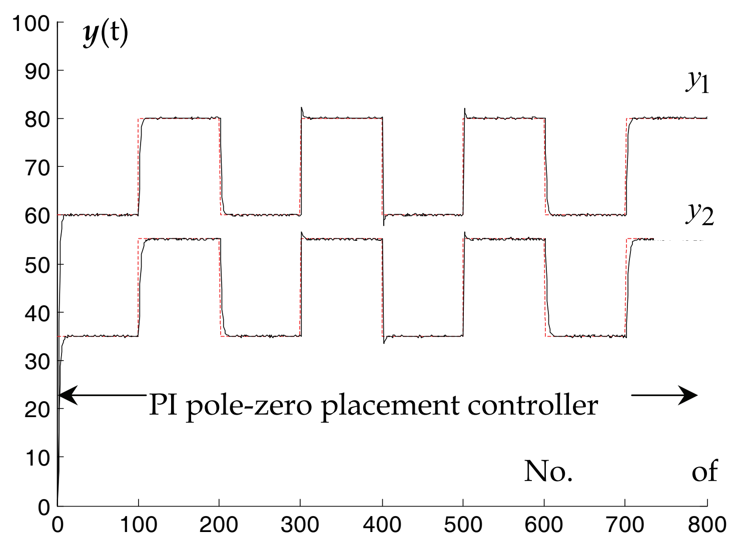


$\mathbf{V} = \begin{bmatrix} 0.1 & 0 \\ 0 & 1.2 \end{bmatrix}$, $\mathbf{P}_{n_1} = \begin{bmatrix} -0.3 & 0 \\ 0 & -0.4 \end{bmatrix}$,
$\mathbf{P}_{d_1} = \begin{bmatrix} -0.8 & 0 \\ 0 & -0.9 \end{bmatrix}$,
$\mathbf{T}_1 = \begin{bmatrix} -0.5 & 0 \\ 0 & -0.6 \end{bmatrix}$
and $\mathbf{T}_2 = \begin{bmatrix} 0 & 0 \\ 0 & 0 \end{bmatrix}$.
The desired zero- placement polynomial matrix $\tilde{\mathbf{h}}$ changes according to equation (48).

Fig. (8a). The outputs

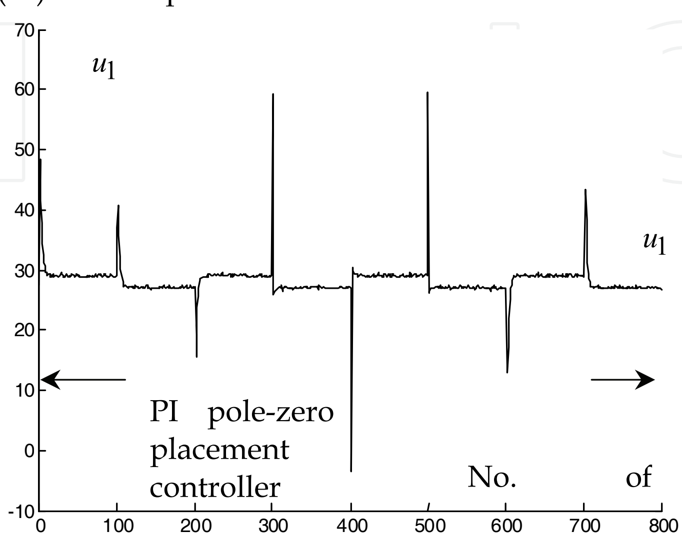


$\mathbf{V} = \begin{bmatrix} 0.1 & 0 \\ 0 & 1.2 \end{bmatrix}$, $\mathbf{P}_{n_1} = \begin{bmatrix} -0.3 & 0 \\ 0 & -0.4 \end{bmatrix}$,
$\mathbf{P}_{d_1} = \begin{bmatrix} -0.8 & 0 \\ 0 & -0.9 \end{bmatrix}$, $\mathbf{T}_1 = \begin{bmatrix} -0.5 & 0 \\ 0 & -0.6 \end{bmatrix}$
and $\mathbf{T}_2 = \begin{bmatrix} 0 & 0 \\ 0 & 0 \end{bmatrix}$.
The desired zero- placement polynomial matrix $\tilde{\mathbf{h}}$ changes according to equation (48).

Fig. (8b) The control input

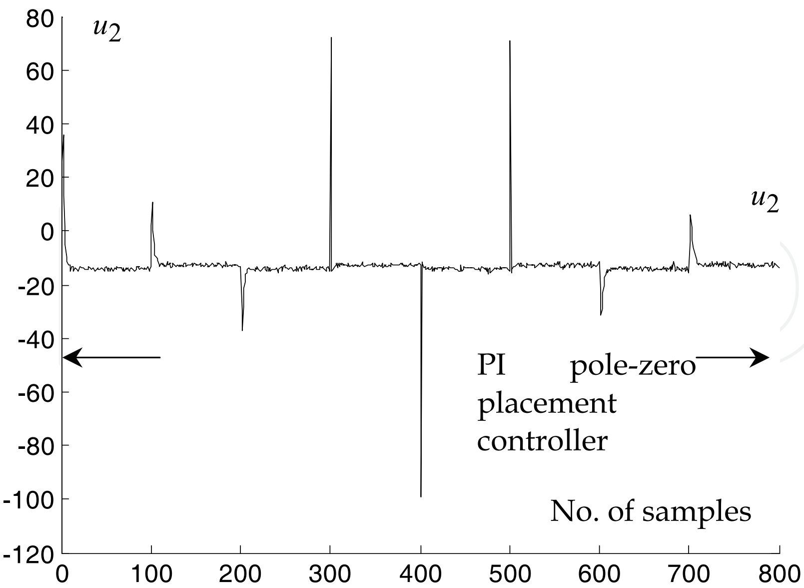

Fig. (8c). The control input

$\mathbf{V}=\begin{bmatrix}0.1 & 0\\ 0 & 1.2\end{bmatrix}$, $\mathbf{P}_{n_1}=\begin{bmatrix}-0.3 & 0\\ 0 & -0.4\end{bmatrix}$,

$\mathbf{P}_{d_1}=\begin{bmatrix}-0.8 & 0\\ 0 & -0.9\end{bmatrix}$,

$\mathbf{T}_1=\begin{bmatrix}-0.5 & 0\\ 0 & -0.6\end{bmatrix}$

and $\mathbf{T}_2=\begin{bmatrix}0 & 0\\ 0 & 0\end{bmatrix}$.

The desired zero- placement polynomial matrix $\tilde{\mathbf{h}}$ changes according to equation (46).

### 3.1.4 Investigating the Influence of the Polynomial $\mathbf{T}$ on the Closed loop Performance Using Implicit Controller

In order to see the effect of the desired closed loop poles polynomial, on the closed loop system performance, the implicit PI pole-zero placement was switched on from $t=0$ to $t=800$ and the zero placement polynomial matrix $\tilde{\mathbf{H}}=[\mathbf{I}+\tilde{\mathbf{h}}]^{-1}(\mathbf{I}+\tilde{\mathbf{h}}_1 z^{-1})$ was fixed, whereas, the polynomial matrix $\mathbf{T}(z^{-1})=\mathbf{I}+\mathbf{T}_1 z^{-1}+\mathbf{T}_2 z^{-2}$ was changed three times as follows:

$$
\begin{aligned}
&0 \le t < 250 && \mathbf{T}=\mathbf{I}+\begin{bmatrix}-.7 & 0\\ 0 & -1.65\end{bmatrix}z^{-1}+\begin{bmatrix}0 & 0\\ 0 & 0.7870\end{bmatrix}z^{-2}\\
&250 \le t < 550 && \mathbf{T}=\mathbf{I}+\begin{bmatrix}-0.8 & 0\\ 0 & -0.95\end{bmatrix}z^{-1}+\begin{bmatrix}0 & 0\\ 0 & 0\end{bmatrix}z^{-2}\\
&550 \le t < 800 && \mathbf{T}=\mathbf{I}+\begin{bmatrix}-1.85 & 0\\ 0 & -0.9\end{bmatrix}z^{-1}+\begin{bmatrix}0.887 & 0\\ 0 & 0\end{bmatrix}z^{-2}
\end{aligned}
\tag{49}
$$

The polynomial $\tilde{\mathbf{h}}$ is selected as follows:

$$\tilde{\mathbf{h}}(z^{-1})=\mathbf{I}+\begin{bmatrix}0.9 & 0\\ 0 & 0.9\end{bmatrix}z^{-1}$$

The outputs and the control inputs are shown in the Figures (9a) and (9b) respectively.
It clear from the Figures (9a) and (9b) that the performance of the closed loop system is affected by the changes in the polynomial $\mathbf{T}$.

### 3.2 Case study 2: Non-minimum Phase System

The implicit PID based pole-zero placement for MIMO systems proposed in section (2.2) is applied to the following MIMO plant, originally introduced by Prager and Wellstead (1980) and treated previously by Zayed et al.(2004) :

$$(\mathbf{I}+\mathbf{A}_1 z^{-1}+\mathbf{A}_2 z^{-2})\mathbf{y}(t)=z^{-1}(\mathbf{B}_0+\mathbf{B}_1 z^{-1})\mathbf{u}(t)+(\mathbf{I}+\mathbf{C}_1 z^{-1})\xi(t) \tag{50}$$

where:

$$\mathbf{A}_1=\begin{bmatrix}-1.4 & -0.2\\ -0.1 & -0.9\end{bmatrix},\ \mathbf{A}_2=\begin{bmatrix}0.48 & 0.1\\ 0 & 0.2\end{bmatrix},\ \mathbf{B}_0=\begin{bmatrix}1 & 0\\ 0 & 0\end{bmatrix},\ \mathbf{B}_1=\begin{bmatrix}1.5 & 1\\ 0 & 1\end{bmatrix},\ \mathbf{C}_1=\begin{bmatrix}-0.5 & 0\\ 0.1 & -0.3\end{bmatrix}$$

and $\xi(t)$ is a white noise vector sequence with zero mean and variance $\mathbf{R}'=\begin{bmatrix}0.1 & 0\\ 0 & 0.1\end{bmatrix}$.

Notice that the plant is a non-minimum phase system and also has different time delays in the two channels.

The set point $\mathbf{w}(t)$ changes every 100 samples as follows:

1. $w_1(t)$ changes from 5 to 10 and from 10 to 5.
2. $w_2(t)$ changes from 15 to 20 and from 20 to 15.

The user-defined gain and the pre-filter polynomials were respectively selected as:

$$\mathbf{V}=\begin{bmatrix}V_1 & 0\\ 0 & V_2\end{bmatrix}=\begin{bmatrix}0.02 & 0\\ 0 & 0.04\end{bmatrix},\ \mathbf{P}_d(z^{-1})=\mathbf{I}+\mathbf{P}_{d_1}z^{-1} \text{ and } \mathbf{P}_n(z^{-1})=\mathbf{I}+\mathbf{P}_{n_1}z^{-1}$$

where $\mathbf{P}_{d_1}(z^{-1})=\begin{bmatrix}-0.5 & 0\\ 0 & -0.6\end{bmatrix}$ and $\mathbf{P}_{n_1}(z^{-1})=\begin{bmatrix}-0.4 & 0\\ 0 & -0.4\end{bmatrix}$.

It can clearly be seen from equations (13a), (15a), (15b) and (15c), that a PID controller is obtained if the polynomial matrix $\overline{\mathbf{F}}_s'$ is of second order. This can be achieved by selecting the pre-filter polynomial matrix $\mathbf{P}_d(z^{-1})$ to be of order one.

The desired closed loop poles and zeros polynomial matrices are respectively selected as follows:

$$\mathbf{T}=\mathbf{I}+\begin{bmatrix}-0.5 & 0\\ 0 & -0.6\end{bmatrix}z^{-1} \text{ and } \tilde{\mathbf{h}}=\mathbf{I}+\begin{bmatrix}0.8 & 0\\ 0 & 0.85\end{bmatrix}z^{-1}.$$

The outputs and the control inputs are, respectively, shown in Figures (10a) and (10b). We can see clearly from these Figures (10a) and (10b) that the excessive control actions resulting from set point changes are further reduced (i.e. more effectively tuned) when the new PID pole-zero placement controller is on line (during thesampling interval 251-550). Small oscillations can also be seen in the control inputs and closed loop system outputs during the last 250 samples (551-800 sampling times), where the conventional self-tuning PID is operating. The performance of the conventional PID controller can be further improved by adjusting the gain matrix $V$ and the user defined polynomial matrices $\mathbf{P}_d$ and $\mathbf{P}_n$. However these tuning parameters must be selected using a trial and error procedure

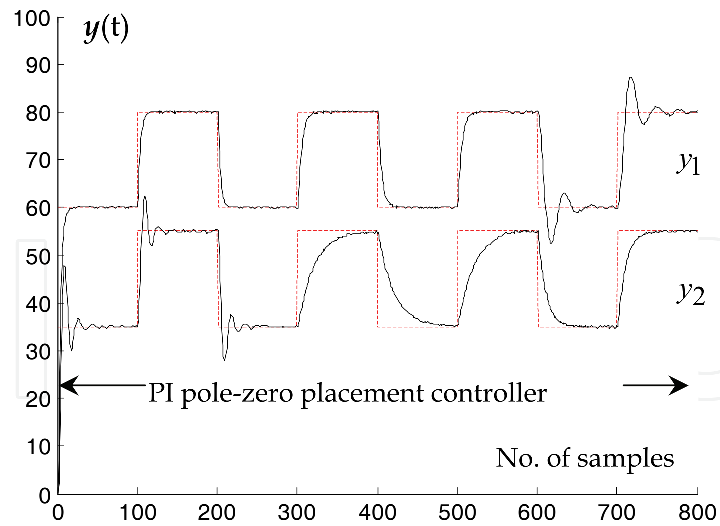


$\mathbf{V}=\begin{bmatrix}0.1 & 0\\ 0 & 1.2\end{bmatrix}$, $\tilde{\mathbf{h}}_1=\begin{bmatrix}0.9 & 0\\ 0 & 0.8\end{bmatrix}$ and $\tilde{\mathbf{h}}_2=\begin{bmatrix}0 & 0\\ 0 & 0\end{bmatrix}$. The polynomial matrix $\mathbf{T}$ changes according to equation (49).

Fig. (9a). the outputs

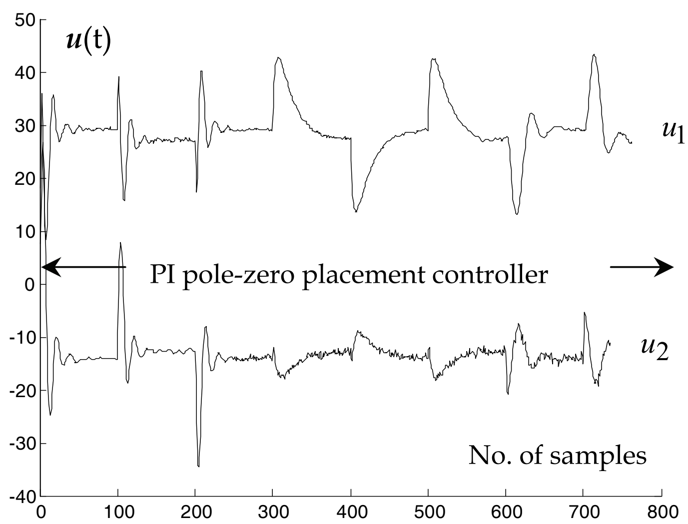


$\tilde{\mathbf{h}}_1=\begin{bmatrix}0.9 & 0\\ 0 & 0.9\end{bmatrix}$ and $\tilde{\mathbf{h}}_2=\begin{bmatrix}0 & 0\\ 0 & 0\end{bmatrix}$. The polynomial matrix $\mathbf{T}$ changes according to equation (49).

–

Fig. (9b). the control inputs

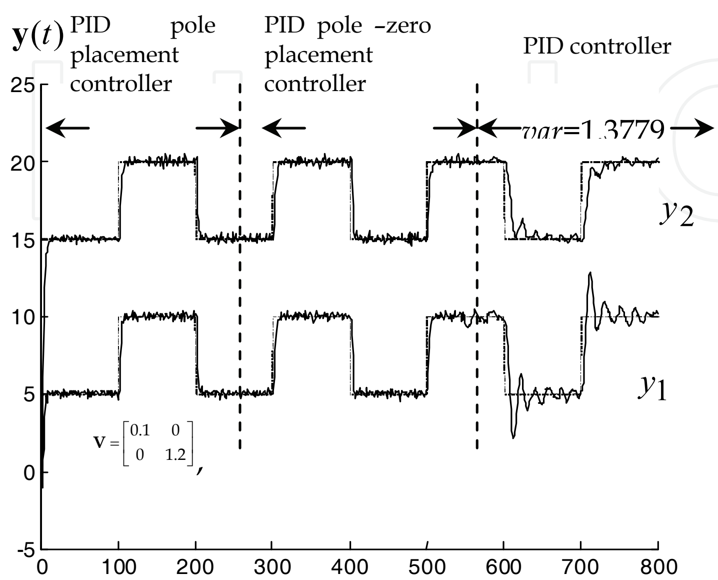


$\mathbf{V}=\begin{bmatrix}0.02 & 0\\ 0 & 0.04\end{bmatrix}$, $\mathbf{P}_{n_1}=\begin{bmatrix}-0.4 & 0\\ 0 & -0.4\end{bmatrix}$, $\mathbf{P}_{d_1}=\begin{bmatrix}-0.5 & 0\\ 0 & -0.6\end{bmatrix}$, $\mathbf{T}_1=\begin{bmatrix}-0.5 & 0\\ 0 & -0.6\end{bmatrix}$ and $\mathbf{T}_2=\begin{bmatrix}0 & 0\\ 0 & 0\end{bmatrix}$. $\tilde{\mathbf{h}}_1=\begin{bmatrix}0.8 & 0\\ 0 & 0.85\end{bmatrix}$ and $\tilde{\mathbf{h}}_2=\begin{bmatrix}0 & 0\\ 0 & 0\end{bmatrix}$.

Fig. (10a). The outputs

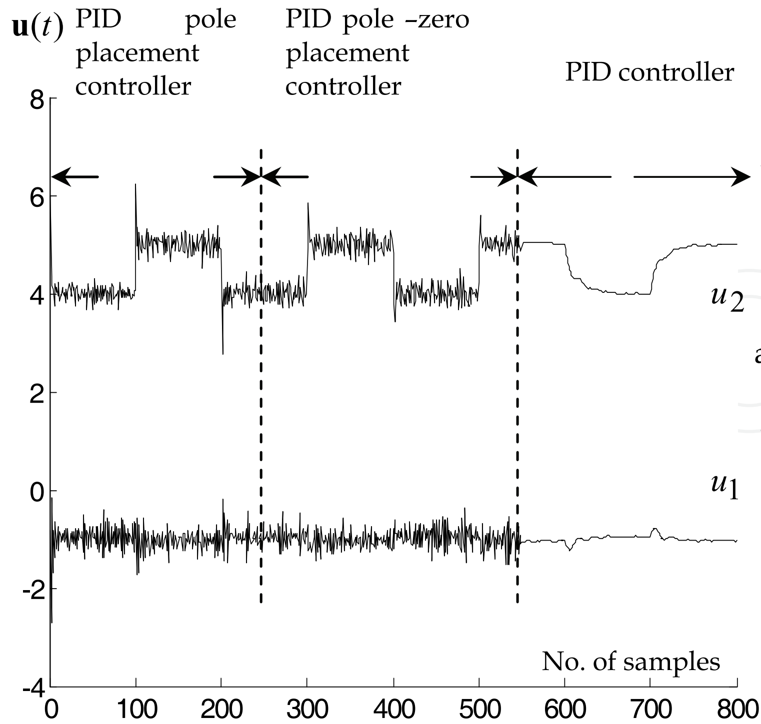


$\mathbf{V} = \begin{bmatrix} 0.02 & 0 \\ 0 & 0.04 \end{bmatrix}$, $\mathbf{P}_{n_1} = \begin{bmatrix} -0.4 & 0 \\ 0 & -0.4 \end{bmatrix}$, $\mathbf{P}_{d_1} = \begin{bmatrix} -0.5 & 0 \\ 0 & -0.6 \end{bmatrix}$, $\mathbf{T}_1 = \begin{bmatrix} -0.5 & 0 \\ 0 & -0.6 \end{bmatrix}$ and $\mathbf{T}_2 = \begin{bmatrix} 0 & 0 \\ 0 & 0 \end{bmatrix}$. $\tilde{\mathbf{h}}_1 = \begin{bmatrix} 0.8 & 0 \\ 0 & 0.85 \end{bmatrix}$ and $\tilde{\mathbf{h}}_2 = \begin{bmatrix} 0 & 0 \\ 0 & 0 \end{bmatrix}$.

Fig. (10b). The control inputs

#### 3.2.1 Investigating the Influence of the load disturbances on the Closed Loop Performance Using the Implicit Controller

The next task is to investigate the influence of the load disturbances on the closed loop system. Constant load disturbances of value $\begin{bmatrix} 1 \\ 1 \end{bmatrix}$ were added to the outputs from the 350th instant to 800th sampling time instant. The two controller set points were both kept constant at values of 10 and 20 throughout.

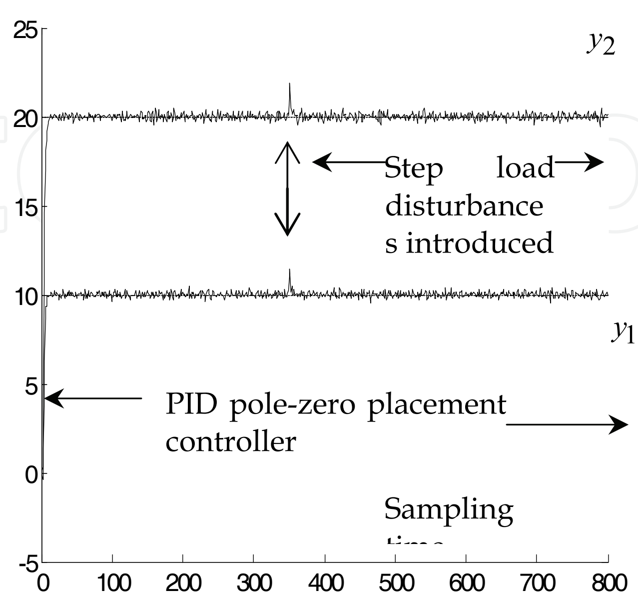


Fig. (11a). The outputs

The outputs and the control inputs for each of the three controller modes (namely PID pole-placement, PID pole-zero placement and the PID controller modes) are shown in the Figures (11a) to (11b) respectively.
It can clearly be seen from all the figures (11a) and (11b) that at steady state, the proposed PID based pole-zero placement controller has the ability to effectively regulate constant load disturbances to zero.

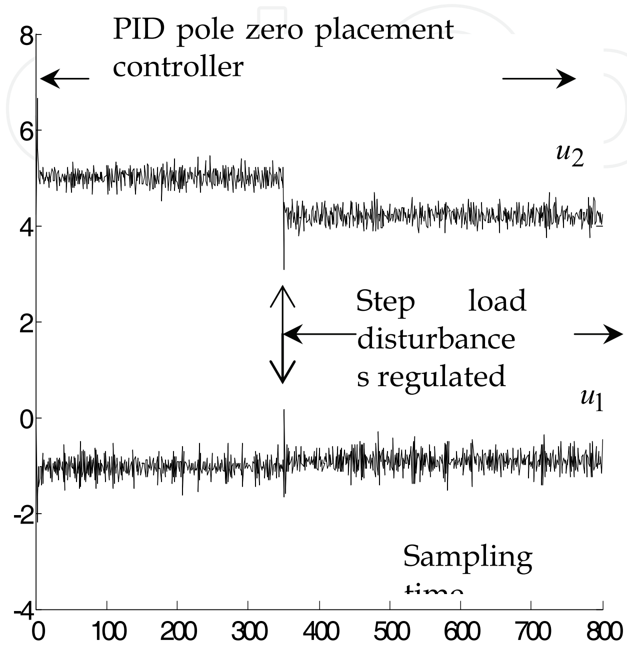


Fig. (11b). The control inputs

## 4. Conclusions

In this chapter, a new computationally efficient algorithm to incorporate the robustness of PID control and classical pole-zero placement into the generalised minimum variance stochastic self-tuning controller for multivariable systems has been proposed. The resulting PID self-tuning controller provides an adaptive mechanism, which ensures that the closed loop poles and zeros are located at their pre-specified positions. It is effectively an implicit algorithm in the sense that the controller design step is trivial (solving Diophantine equation at each sampling instant is avoided). Furthermore, the results presented here indicate that the controller tracks set point changes with the desired speed of response, penalises the excessive control action, and can deal with non-minimum phase systems. The transient response is shaped by the choice of the pole polynomial $\mathbf{T}(z^{-1})$, while the zeropolynomial $\tilde{\mathbf{H}}'(z^{-1})$ can be used to reduce the magnitude of control action or to achieve better set point tracking. In addition, the controller has the ability to ensure zero steady state error. Moreover, the controller is obtained as a left matrix-fraction and so can be immediately implemented. It is clear from sections (2.1), (2.2) and (3.3) that the proposed control design can be extended to a novel implicit multiple PID control. In this case the controller can then be operated in three modes, as either a conventional PID self-tuning controller, an implicit pole placement self-tuning control or a newly proposed implicit PID pole-zero placement controller through the flick of a switch. The switching decision between the different PID controllers can be done manually or by using stochastic learning Automata.

## 5. References

Yusof R. & et al., (1994). Self-tuning PID control: a multivariable derivation and application, *Automatica*, *30*, pp. 1975-1981.

Yusof, R.; (1993). A multivariable self-tuning PID controller, *Int. J. Control, 57*, pp.1387-1403.

Tokuda M.; & Yamamoto T.; (2002) A neural-Net Based Controller supplementing a Multiloop PID Control System, *IEICE Trans. Fundamentals, Vol. E85-A*, 1, pp256-261.

Zayed, A. & et al., (2004). A New Multivariable Generalised Minimum-variance Stochastic Self-tuning with Pole-zero Placement, *International Journal of Control and Intelligent Systems*, *32* (1), pp2004, 35-44.

Sirisena H. & Teng F.,(1986). Multivariable pole-zero placement self-tuning controller, *Int. J. Systems Sci*., *17*(2), pp. 345-352.

Zhu Q., & et al., (2002)., A neural network enhanced generalised minimum variance self-tuning proportional, integral and derivative control algorithm for complex dynamic systems, *Journal of systems and Control Engineering, 216, part 1*, pp. 265-273.

Zayed A. & Hussain A., (2004). A New multivariable Non-linear Multiple-Controller Incorporating a Neural Network Learning Sub-model, *The first International Conference on Brain Inspired Cognitive Systems*, Stirling, Scotland, Uk., 29 Aug.-1 Sep., paper in CD.

Astrom K.., & Wittenmark B., (1973) On self-tuning regulators, *Automatica*, *9*, pp.185-199.

Prager D., & wellstead P., Multivariable pole-placement Self-tuning regulators, *Proc. Inst. Electr. Engineering*, *Part D*, *128*, 1980, 9-18.

Zayed A., (1997) *Minimum Variance Based Adaptive PID Control Design*, M.Phil Thesis, Industrial Control Centre, University of Strathclyde, Glasgow, U.K.

Zayed A., (2005) *Novel linear and nonlinear minimum variance control techniques for adaptive control engineering*, PhD Thesis , Department of computing science and mathematics, University of Stirling, U.K.

Zayed A.,& et al., (2006). A novel multiple-controller incorporating a radial basis function neural networks based generalised learning model, *Neurocomputing,69,* pp.1868-1881.

Yusof R.,& et al (1994), Temperature control of a water bath by self-tuning PI controller, *INT. J. SYSTEMS SCI., 25*, pp1391-1404.

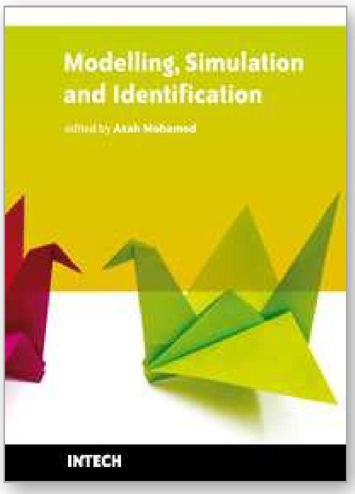


**Modelling, Simulation and Identification**

Edited by Azah Mohamed

ISBN 978-953-307-136-7
Hard cover, 354 pages
**Publisher** Sciyo
**Published online** 18, August, 2010
**Published in print edition** August, 2010

Modeling, simulation and identification has been actively researched in solving practical engineering problems. This book presents the wide applications of modeling, simulation and identification in the fields of electrical engineering, mechanical engineering, civil engineering, computer science and information technology. The book consists of 17 chapters arranged in an order reflecting multidimensionality of applications related to power system, wireless communication, image and video processing, control systems, robotics, soil mechanics, road engineering, mechanical structures and workforce capacity planning. New techniques in signal processing, adaptive control, non-linear system identification, multi-agent simulation, eigenvalue analysis, risk assessment, modeling of dynamic systems, finite difference time domain modeling and visual feedback are also presented. We hope that readers will find the book useful and inspiring by examining the recent developments in the applications of modeling, simulation and identification.